

**SPECTRAL CHARACTERIZATION OF DESICCATED PHYLLOSILICATE SAMPLES AS ANALOGUES FOR PHOBOS AND PRIMITIVE SOLAR SYSTEM BODIES.** K. L. Donaldson Hanna<sup>1</sup>, T. Warren<sup>1</sup>, and N. E. Bowles<sup>1</sup>, <sup>1</sup>Atmospheric, Oceanic and Planetary Physics, University of Oxford, Oxford, UK (Kerri.DonaldsonHanna@physics.ox.ac.uk).

**Introduction:** The surface of Phobos holds many keys for understanding its formation and evolution as well as the history and orbital dynamics of the Mars system. Visible to near infrared (VNIR) telescopic and spacecraft observations suggests that Phobos' surface is compositionally heterogeneous with 'redder' and 'bluer' units that both appear to be anhydrous in nature [e.g. 1-7]. VNIR spectra of both spectral units lack strong diagnostic absorptions making it difficult to assess surface mineralogy or develop analogue materials. Suggested VNIR spectral analogues include a range of materials: mature lunar highlands, carbonaceous chondrites, laboratory-heated carbonaceous chondrites, thermally metamorphosed CI/CM chondrites, desiccated phyllosilicates, and highly space weathered mafic mineral assemblages [e.g. 1-9]. Unlike the VNIR, thermal infrared (TIR) observations of Phobos' surface suggest that TIR spectral measurements include diagnostic spectral features. The identification of these spectral features suggests the regolith of Phobos could include phyllosilicates (clays) and tectosilicates (feldspars) [e.g. 10-12].

In this initial study we desiccate phyllosilicate samples in an effort to characterize thermal infrared spectral differences between typical phyllosilicate sample material and desiccated sample material under Earth-like and Phobos-like conditions. These new measurements will enable the interpretation of current and future remote sensing observations of Phobos and other primitive solar system bodies as desiccating surface conditions are not limited to Phobos.

**Experimental Methods:** Fe-bearing, Al-poor nontronite (NAu-2) sourced from the Clay Minerals Society was crushed and sieved to particle sizes spectrally dominant in the regolith of airless bodies (< 25  $\mu\text{m}$ ). Sample material was desiccated by heating the sample to 200°C in a box purged with nitrogen gas ( $\text{N}_2$ ), keeping the relative humidity < 0.1%, for 72 hours. Morris et al. [13] demonstrated that similar experimental conditions were effective in removing the interlayer  $\text{H}_2\text{O}$  in two nontronite samples. Near infrared (NIR) reflectance measurements and X-Ray diffraction (XRD) measurements were made on nontronite and desiccated nontronite to confirm the removal of the  $\text{H}_2\text{O}$  interlayer. An image of nontronite and desiccated nontronite loaded into NIR sample cups can be seen in Figure 1. NIR measurements were made with a Bruker IFS66v Fourier Transform Infrared (FTIR) spectrom-

eter in the Planetary Spectroscopy Facility (PSF) at the University of Oxford and the XRD measurements were made in the Department of Physics at the University of Oxford.

Thermal infrared emissivity measurements were made under ambient (Earth-like) and a Simulated Phobos Environment (SPE) using the Simulated Lunar Environment Chamber (SLEC) in the PSF at Oxford. The experimental setup and calibration of SLEC has been described by Thomas et al. [14]. Under ambient conditions, samples are heated from below to 80°C while the environment chamber is at ambient pressure (~1000 mbar) and temperature (~28 K). The near surface environment of Phobos is simulated by: (1) removing atmospheric gases from inside the chamber (<  $10^{-4}$  mbar), (2) cooling the interior of the chamber to < 100 K, and (3) heating the samples from below and above until the brightness temperature of the sample is ~320 K. Samples are heated from below using heaters embedded in the base of each sample cup and from above using solar-like halogen lamps. Radiation emitted from the sample is reflected into a Bruker IFS66v FTIR spectrometer by a collecting mirror positioned above the sample. Spectral measurements are collected at a resolution of 2-4  $\text{cm}^{-1}$  over the ~400 – 2400  $\text{cm}^{-1}$  spectral range.

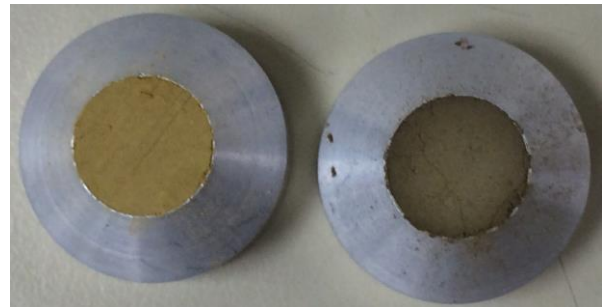


**Figure 1.** Image of nontronite (left) and desiccated nontronite (right) loaded into NIR sample cups.

**NIR Results:** NIR spectra of nontronite are affected by the removal of the  $\text{H}_2\text{O}$  interlayer as seen in Figure 2. After 72-hours of high temperature and low atmospheric  $\text{H}_2\text{O}$  concentration, the absorption bands near 1.4 and 1.9  $\mu\text{m}$  (owing to the fundamental stretching and bending vibrations of the  $\text{H}_2\text{O}$  molecule [15]) are greatly reduced as is the 2.7 – 3.1  $\mu\text{m}$  region (owing to water and OH-stretching vibrations [15]). The diagnostic absorption bands near 2.29, 2.4 and 2.50  $\mu\text{m}$  [e.g. 16] are at the same wavelengths in the nontronite

and desiccated nontronite spectra and are of similar depth. The desiccated nontronite spectrum has a reddened slope between 1 and 1.8  $\mu\text{m}$  and is likely due to the change in albedo of the sample as it is heated and volatiles are removed (Figure 1). These results corroborate earlier work by Morris et al. [13].

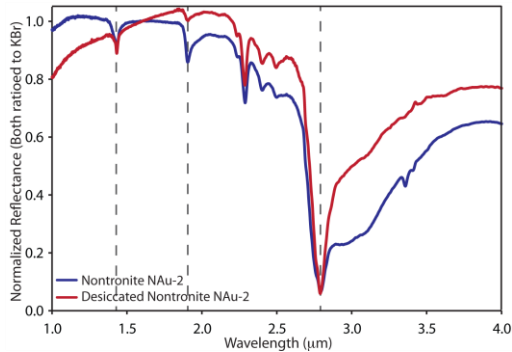


**Figure 2.** NIR spectra of nontronite (NAu-2) and desiccated nontronite (NAu-2). Both nontronite samples are of the <25  $\mu\text{m}$  particle size fraction.

**TIR Results:** Ambient or ‘Earth-like’ TIR measurements of nontronite and desiccated nontronite are shown in the top plot of Figure 3. Spectral features related to silicate mineralogy in the  $\sim 1250$  to  $400\text{ cm}^{-1}$  spectral range are observed at the same frequencies ( $\text{cm}^{-1}$ ) and with similar band depths. However, in the  $\text{H}_2\text{O}$ -bending band region of the spectrum ( $\sim 1620$  –  $1650\text{ cm}^{-1}$ ) differences are observed in band positions and band depths between the nontronite and desiccated nontronite spectra.

Simulated Phobos environment TIR measurements of nontronite and desiccated nontronite are shown in the bottom plot of Figure 3. Several observations can be made when comparing SPE spectra with ambient spectra: (1) the main emission maximum near  $8\text{ }\mu\text{m}$  called the Christiansen feature shifts to shorter wavelengths under a SPE, (2) the spectral contrast between the Christiansen feature and the fundamental vibration bands between  $\sim 1100$  and  $700\text{ cm}^{-1}$  increases under a SPE, and (3) the absorption features in the  $\text{H}_2\text{O}$ -bending band region are reduced under a SPE. Under a SPE, nontronite and desiccated nontronite spectral features in the  $\sim 1250$  to  $400\text{ cm}^{-1}$  spectral range are observed at the same frequencies ( $\text{cm}^{-1}$ ) and with similar band depths. However, in the  $\text{H}_2\text{O}$ -bending band region of the spectrum differences are observed in band positions and band depths between the nontronite and desiccated nontronite spectra.

**Future Work:** Results from this initial study suggest that only minor effects due to the desiccation of a sample are observed in TIR spectral measurements under ambient and simulated Phobos conditions. However, additional laboratory work needs to be done

to confirm the results presented here and to measure additional phyllosilicate samples within the smectite group and across other phyllosilicate groups. Detailed laboratory studies across multiple spectral ranges, like the one performed in this work, will enable the interpretation of remote sensing observations to better understand surface compositions of Phobos as well as other primitive solar system bodies.

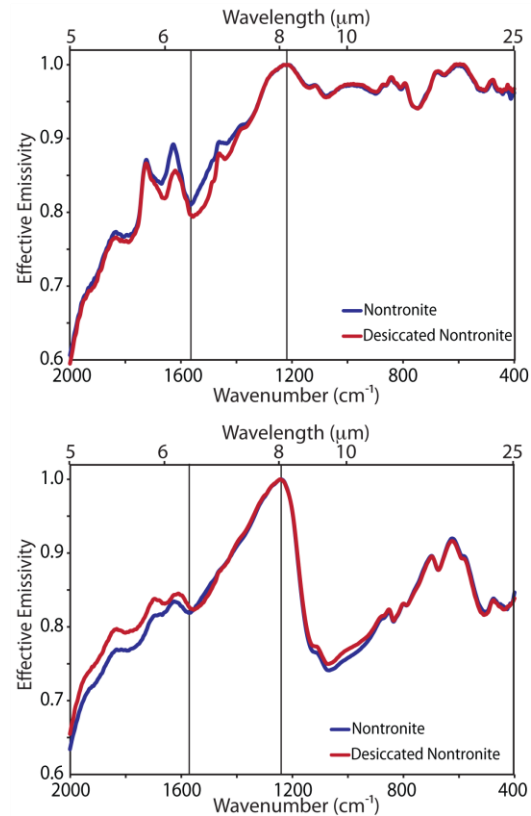


**Figure 3. (Top)** Ambient TIR spectra of nontronite (NAu-2) and desiccated nontronite (NAu-2). **(Bottom)** Simulated Phobos Environment TIR spectra of nontronite (NAu-2) and desiccated nontronite (NAu-2). Both nontronite samples are of the <25  $\mu\text{m}$  particle size fraction

**References:** [1] Pang K. D. et al. (1978) *Science*, 199, 64-66. [2] Pollack J. B. et al. (1978) *Science*, 199, 66-69. [3] Lunine J. L. et al. (1982) *JGR*, 87, 10297-10305. [4] Murchie S. and Erard S. (1996) *Icarus*, 123, 63-86. [5] Rivkin A. S. et al. (2002) *Icarus*, 156, 64-75. [6] Fraeman A. A. et al. (2014) *Icarus*, 229, 196-205. [7] Pieters C. M. et al. (2014) *Planet. & Space Sci.*, 102, 144-151. [8] Hiroi T. et al. (1993) *Science*, 261, 1016-1018. [9] Hiroi T. et al. (2001) *Science*, 293, 2234-2236. [10] Roush T. L. and Hogan R. C. (2001) *LPS XXXII*, Abstract #1915. [11] Giuranna M. et al. (2011) *Planet. & Space Sci.*, 59, 1308-1325. [12] Glotch T. D. and Edwards C. S. (2014) *1<sup>st</sup> Exp. Sci. Forum*. [13] Morris R. V. et al. (2010) *LPS XLI*, Abstract #2156. [14] Thomas I. R. et al. (2012) *Rev. Sci. Instrum.*, 83(12), 124502. [15] Farmer V. C. (1974) *The Infrared Spectra of Minerals*. [16] Bishop J. L. et al. (2008) *Clay Minerals*, 43, 35-54.